Received: 16 April 2018 | Revised: 26 June 2018 | Accepted: 27 June 2018

DOI: 10.1002/aoc.4523

FULL PAPER

WILEY Applied Organometallic Chemistry

Synthesis, characterization and biological applications of some substituted pyrazoline based palladium (II) compounds

Khyati P. Thakor | Miral V. Lunagariya | Bhupesh S. Bhatt | Mohan N. Patel

Department of Chemistry, Sardar Patel University, Vallabh Vidyanagar 388120, Gujarat, India

Correspondence
Mohan N. Patel and Bhupesh S. Bhatt, Department of Chemistry, Sardar Patel University, Vallabh Vidyanagar 388120, Gujarat, India.
Email: jeenen@gmail.com; bhupeshbhatt31@gmail.com

Palladium (II) complexes of the type [$PdLCl_2$] (where L = substituted pyrazoline ligands) have been synthesized. The metal complexes (5a-5f) have been characterized by various spectroscopic and analytical techniques like ^{1}H-NMR, ^{13}C-NMR, LC–MS, IR, Energy-dispersive X-ray (EDX), electronic spectroscopy, thermogravimetric analysis (TGA), elemental analysis and conductance measurement. Complexes to herring sperm DNA (HS-DNA) binding has been explored by absorption titration and binding constant (K_b) as well as Gibb's free energy have been evaluated. Complex 5b shows the highest binding constant value. So, thermodynamic parameters of 5b-HS DNA complex at different temperature have been evaluated. Also, Viscosity measurement and molecular modeling studies have been performed to know the binding mode of complexes. Based on the observations, an intercalative binding mode of DNA has been proposed. Further confirmation of intercalative mode of DNA binding has been taken by fluorescence spectroscopy and results are in a good agreement with absorption titration, viscosity measurement and molecular modeling data. Antibacterial activity of the complexes has been screened against pathogenic bacteria such as *S. aureus, E. coli, B. subtilis, S. marcescens* and *P. aeruginosa*. Cytotoxicity is performed on brine shrimp and *S. pombe*. Gel electrophoresis assay demonstrates that all the complexes can cleave the pUC19 plasmid DNA. Anti-tuberculosis activity has been carried out using mycobacterium tuberculosis H_{37}Rv bacteria by L.J. Medium conventional method.

KEYWORDS
cytotoxicity, DNA intercalation, ethidium bromide displacement, free energy, mycobacterium tuberculosis

1 | INTRODUCTION

The *d*-block metal complexes that cleave DNA under physiological condition are of current interest in the development of artificial nucleases.[1,2] Phosphodiester hydrolysis with the cooperation of metal ions and the functional group is one of the approaches to design multifunctional metal complexes.[3,4] The site specific DNA cleavage by newly designed metal complexes allow the development of new antimicrobial agents as well as chemotherapeutic agents.[5–7] The metal complexes are well suited as artificial metallonuclease due to the

applications associated with different geometries and the possibility to tune their redox potential by choosing proper ligands.[8] Many organic molecules have been designed to consolidate biological functional group with a suitable metal ion to mimic active sites of metalloproteins.[9] Thus, the efficiency of DNA cleavage can be enhanced through promising coordination compound typically contain a DNA binding group that fit to either major groove or minor groove, and/or may act as intercalator, thereby increasing DNA target ability of the coordination compounds.[10–13] 4, 5-Dihydropyrazoles, a small bioactive molecule, are pre-eminent structural design found in numerous pharmaceutically active compounds (antifungal, antibacterial, anti-tumour, anti-inflammatory and antiviral) and agrochemical active agents.[14–17] The combination of transition metals with biologically active molecules has also been exploited showing promising activity due to their unique ability to bind different biological targets.[18]

Platinum based anticancer drug has several side effects like nephrotoxicity and drug resistance of tumour cells, which have generated real challenges to researchers.[19,20] Several side effect along with limited applicability to certain cell lines associated with cisplatin administration have triggered the research in the development of other transition metal based drugs.[21–24] Morphology, geometry, electronic state of palladium metal ion is very similar to platinum metal ion. Also, palladium based metal complexes have been extensively researched for diverse biological and pharmacological applications.[25–34] Thus, platinum analogous palladium compounds have been designed and synthesized, which show promising activity against tumour cell line.[35]

So to explore biochemistry of palladium metal, we have synthesized 1,3,5-trisubstituted pyrazoline ligands and their chelation with palladium (II) has been carried out. All synthesized compounds have been screened for the various biological activity like antibacterial activity, cytotoxicity, DNA binding and DNA cleavage.

2 | EXPERIMENTAL

2.1 | Materials and reagents

All the chemicals and solvents were of analytical grade (Purity >99%) and used as purchased. Na_2PdCl_4 (98%), 2-acetyl thiophene (≥98%), p-fluorobenzaldehyde (98%), p-chlorobenzaldehyde (97%), p-bromobenzaldehyde (99%), m-chlorobenzaldehyde (97%), m-bromobenzaldehyde (97%), m-fluorobenzaldehyde (97%), potassium tert-butoxide (≥98%), HS DNA and EDTA (≥99%) were purchased from Sigma Aldrich Chemical Co. (India). Agarose, Luria Broth (LB), ethidium bromide (EB), bromophenol blue and xylene cyanol FF were purchased from Himedia (India). S. pombe Var. Paul Linder 3360 was obtained from IMTECH, Chandigarh.

2.2 | Physical measurement

C, H, and N elemental analyses were performed with a model EURO EA3000 Elemental Analyser. The ^{1}H NMR (400 MHz) and ^{13}C NMR (100 MHz) spectra were recorded with a Bruker Avance. IR spectra were recorded on a FT-IR Shimadzu spectrophotometer with sample prepared as KBr pellets in the range 4000–400 cm^{-1}. Precoated silica gel plates (silica gel 0.25 mm, 60 G F 254; Merck, Germany) were used for thin layer chromatography. The LC–MS spectra were recorded using Thermo scientific mass spectrophotometer (USA). The electronic spectra were recorded on a UV-160A, UV–vis spectrophotometer, Shimadzu, Kyoto (Japan). The magnetic moments were measured by Gouy's method using mercury tetrathiocyanatocobaltate (II) as the calibrant ($\chi_g = 16.44 \times 10^{-6}$ cgs units at 20 °C), citizen balance. Antibacterial study was carried out using laminar air flow cabinet Toshiba, Delhi (India). The thermogram of complexes was recorded with a SDT Q600 V20.9 Build 20 thermogravimetric analyser. Conductance measurement was carried out using conductivity meter model number E-660A. Ethidium bromide displacement experiments were performed using Fluoromax-4 spectrofluorometer, Horiba. Photo quantization of the gel after electrophoresis was done using Alpha-DigiDoc™ RT version V.4.0.0 PC-Image software, California (USA).

2.3 | Synthesis of the compounds

2.3.1 | General method for synthesis of α,β-unsaturated ketones (chalcones)(3a-3f)

To a solution of 2-acetyl thiophene (1) (10 mmol, 1.08 mL) in 20 mL of methanol, freshly prepared methanolic KOH solution (10 mmol, 0.56 g) was added, stirred for 15 min and appropriate aldehyde (2a–2f) (10 mmol) was added. The reaction mixture was stirred at room temperature for 2 h. The reaction mixture was poured to ice cooled water and neutralized with dilute hydrochloric acid. The white precipitate was separated by filtration and washed with distilled water to give the crude product. The obtained product was recrystallized from methanol. The purity of the products was checked on TLC by using a mixture of ethyl acetate and hexane (20:80) as the mobile phase.

2.3.2 | General method for synthesis of 1,3,5-trisubstituted pyrazolines (4a-4f)

To a solution of the appropriate enones (**3a**–**3f**) (5 mmol) in 10 mL of methanol, phenyl hydrazine (5 mmol, 0.49 mL) and freshly prepared methanolic potassium tert-butoxide (5 mmol, 0.56 g) solution were added. The reaction mixture was refluxed for 5–6 h. The reaction was monitored in every 60 min interval on precoated silica TLC plates by using a mixture of ethyl acetate and hexane (20:80) as the mobile phase. The reaction mixture was poured into ice cooled water. The products precipitated out at low temperature were washed with an excess of distilled water, and recrystallized in a minimum amount of methanol and dried under reduced pressure. The proposed reaction for the synthesis of ligands 4a–4f is shown in Scheme 1.

5-(4-Bromophenyl)-1-phenyl-3-(thiophen-2-yl)-4, 5-dihydro-1H-pyrazole (4a)

Prepared by above method using (E)-3-(4-bromophenyl)-1-(thiophen-2-yl)prop-2-en-1-one (**3a**) (5 mmol, 1.47 g) and phenyl hydrazine (5 mmol, 0.49 mL). Yield: 70%; yellow crystalline solid. mp: 153–155 °C; mol. wt. 383.31 g mol^{-1}; anal. Calc. for: $C_{19}H_{15}BrN_2S$, calc. (found) (%): C, 59.54 (59.12); H, 3.94 (3.51); N, 7.31 (7.01); S, 8.36 (7.56); ^{1}H NMR (400 MHz, DMSO-d_6) δ/ppm: 3.12 (1H, dd, J = 7.2 Hz, 17.2 Hz, 4-H_a), 3.87 (1H, dd, J = 12.4 Hz, 16.8 Hz, 4-H_b), 5.25 (1H, dd, J = 7.2 Hz, 12.4 Hz, 5-H), 6.80–7.25,7.47–7.50 (11H, m, 3′,4′, 2″,3″,5″,6″,2‴,3‴,4‴, 5‴,6‴-H), 7.34 (1H, q, J = 1.2 Hz, 3.6 Hz, 2'-H); ^{13}C NMR (100 MHz, DMSO-d_6) δ/ppm: 43.99 (-CH_2 of pyrazoline), 62.95 (-CH of pyrazoline), 113.09, 114.30, 116.45, 116.98, 119.28, 128.30, 128.34, 128.43, 128.48, 129.26, 129.33, 141.13 (-CH of aromatic region); 122.34, 132.45, 135.42, 144.03, 144.09 (-C of aromatic region); IR (KBr, 4000–400 cm^{-1}); 3078, υ (C–H)$_{ar\ stretching}$; 1589, υ (C=N); 1311, υ (C=C); 1103, υ (C–N); 1056, υ (C–Br); 1002, 964, (*p*-substituted aromatic ring); 748, υ (C–H)$_{ar\ bending}$; 871, υ (C-S-C)$_{tiophene}$; Mass (*m/z*%): 383 (100) [M^+]; UV–vis: λ (nm) (ε, M^{-1} cm^{-1}): 263 (155200), 378 (174100).

5-(3-Bromophenyl)-1-phenyl-3-(thiophen-2-yl)-4, 5-dihydro-1H-pyrazole (4b)

Prepared by above method using (E)-3-(3-bromophenyl)-1-(thiophen-2-yl)prop-2-en-1-one (3b) (5 mmol, 1.47 g) and phenyl hydrazine (5 mmol, 0.49 mL). Yield: 69%; yellow crystalline solid. mp: 154–156 °C; mol. wt. 383.31 g mol^{-1}; anal. Calc. for: $C_{19}H_{15}BrN_2S$, calc. (found) (%): C, 59.54 (59.05); H, 3.94 (3.42); N, 7.31 (7.25); S, 8.36 (7.28); ^{1}H NMR (400 MHz, DMSO-d_6) δ/ppm: 3.17 (1H, dd, J = 6.8 Hz, 17.2 Hz, 4-H_a), 3.93 (1H, dd, J = 12.0 Hz, 17.6 Hz, 4-H_b), 5.53 (1H, dd, J = 6.0 Hz, 11.6 Hz, 5-H), 6.73–7.51 (11H, m, 3′,4′,2″,3″,4″,6″,2‴, 3‴,4‴,5‴,6‴-H), 7.62 (1H, d, J = 5.6 Hz, 2'-H); ^{13}C NMR (100 MHz, DMSO-d_6) δ/ppm: 44.09 (-CH_2 of pyrazoline), 62.98 (-CH of pyrazoline), 113.40, 114.44, 119.37, 123.02,, 128.12, 128.20, 128.32, 128.44, 129.13, 129.49, 130.90, 131.80 (-CH of aromatic region); 122.62, 125.38, 135.89, 144.37, 145.46 (-C of aromatic region); IR (KBr, 4000–400 cm^{-1}); 3080, υ (C–H)$_{ar\ stretching}$; 1589, υ (C=N); 1315, υ (C=C); 1109, υ (C–N); 1058, υ (C–Br); 890, (*m*-substituted aromatic ring); 750, υ (C–H)$_{ar\ bending}$; 867, υ (C-S-C)$_{tiophene}$, Mass (*m/z*%): 383 (100) [M^+]; UV–vis: λ (nm) (ε, M^{-1} cm^{-1}): 266 (199400), 375 (239900).

5-(4-Fluorophenyl)-1-phenyl-3-(thiophen-2-yl)-4, 5-dihydro-1H-pyrazole (4c)

Prepared by above method using (E)-3-(4-fluorophenyl)-1-(thiophen-2-yl)prop-2-en-1-one (3c) (5 mmol, 1.16 g) and phenyl hydrazine (5 mmol, 0.49 mL). Yield: 80%; yellow crystalline solid. mp: 158–160 °C; mol. wt. 322.40 g mol^{-1}; ^{1}H NMR (400 MHz, DMSO-d_6) δ/ppm:

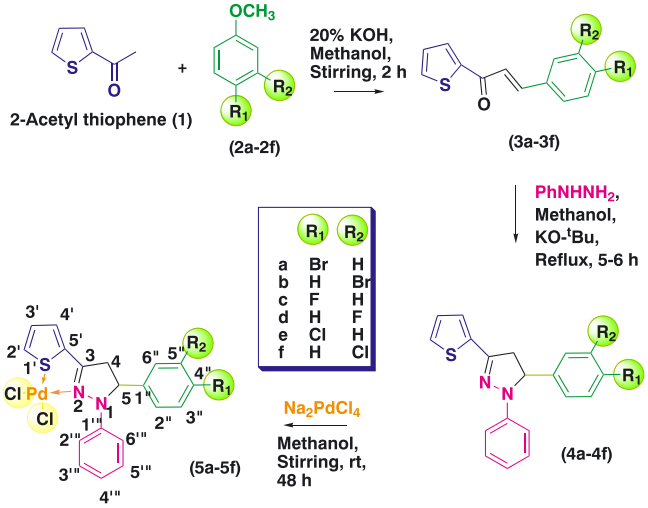

SCHEME 1 Outline of general synthesis of compounds (5a-5f)

3.13 (1H, dd, J = 6.0 Hz, 17.2 Hz, 4-H_a), 3.92 (1H, dd, J = 12.4 Hz, 17.6 Hz, 4-H_b), 5.52 (1H, dd, J = 6.0 Hz, 12.0 Hz, 5-H), 6.71–7.06 (11H, m, 3′,4′, 2″,3″,5″,6″,2‴, 3‴,4‴,5‴,6‴-H), 7.62 (1H, d, J = 4.8 Hz, 2'-H); ^{13}C NMR (100 MHz, DMSO-d_6) δ/ppm: 44.13 (-CH_2 of pyrazoline), 62.95 (-CH of pyrazoline), 113.43, 114.40, 116.17, 116.38, 119.23, 128.04, 128.30, 128.37, 128.45, 129.40, 129.58, 131.38 (-CH of aromatic region); 122.13, 138.88, 144.21, 144.39, 163.05 (-C of aromatic region); IR (KBr, 4000–400 cm^{-1}); 3070, υ (C–H)$_{ar\ stretching}$; 1589, υ (C=N); 1319, υ (C=C); 1149, υ (C–N); 1060, υ (C–Cl); 1003, 964, (*p*-substituted aromatic ring); 748, υ (C–H)$_{ar\ bending}$; 872, υ (C-S-C)$_{thiophene}$; Mass (*m/z*%): 322 (100) [M^+]; UV–vis: λ (nm) (ε, M^{-1} cm^{-1}): 260 (75200), 376 (78800).

5-(3-Fluorophenyl)-1-phenyl-3-(thiophen-2-yl)-4, 5-dihydro-1*H*-pyrazole (4d)

Prepared by above method using (E)-3-(3-fluorophenyl)-1-(thiophen-2-yl)prop-2-en-1-one (**3d**) (5 mmol, 1.16 g) and phenyl hydrazine (5 mmol, 0.49 mL). Yield: 82%; yellow crystalline solid. mp: 155–157 °C; mol. wt. 383.31 g mol^{-1}; ^{1}H NMR (400 MHz, DMSO-d_6) δ/ppm: 3.165 (1H, dd, J = 6.0 Hz, 17.2 Hz, 4-H_a), 3.94 (1H, dd, J = 12.0 Hz, 17.2 Hz, 4-H_b), 5.53 (1H, dd, J = 6.4 Hz, 12.4 Hz, 5-H), 6.72–7.43 (11H,m, 3′,4′,2″,3″,4″,6″, 2‴,3‴,4‴,5‴,6‴-H), 7.62 (1H, d, J = 5.2 Hz, 2'-H); ^{13}C NMR (100 MHz, DMSO-d_6) δ/ppm: 42.04 (-CH_2 of pyrazoline), 63.16 (-CH of pyrazoline), 113.12, 113.33, 113.42, 114.72, 114.93, 119.34, 128.07, 128.13, 128.30, 128.45, 131.62, 131.70 (-CH of aromatic region); 122.37, 135.94, 145.62, 145.69, 161.68 (-C of aromatic region); IR (KBr, 4000–400 cm^{-1}); 3072, υ (C–H)$_{ar\ stretching}$; 1587, υ (C=N); 1320, υ (C=C); 1150, υ (C–N); 1059, υ (C–Cl); 940, (*m*-substituted aromatic ring); 747, υ (C–H)$_{ar\ bending}$; 871, υ (C-S-C)$_{thiophene}$; Mass (*m/z*%): 322 (100) [M^+]; UV–vis: λ (nm) (ε, M^{-1} cm^{-1}): 261 (82100), 373 (65500).

5-(4-Chlorophenyl)-1-phenyl-3-(thiophen-2-yl)-4, 5-dihydro-1H-pyrazole (4e)

Prepared by above method using (E)-3-(4-chlorophenyl)-1-(thiophen-2-yl)prop-2-en-1-one (3e) (5 mmol, 1.24 g) and phenyl hydrazine (5 mmol, 0.49 mL). Yield: 86%; yellow crystalline solid. mp: 149–151 °C; mol. wt. 338.85 g mol^{-1}; anal. Calc. for: $C_{19}H_{15}ClN_2S$, calc. (found) (%): C, 67.35 (67.05); H, 4.46 (4.11); N, 8.27 (8.01); S, 9.46 (8.95); ^{1}H NMR (400 MHz, DMSO-d_6) δ/ppm: 3.13 (1H, dd, J = 6.4 Hz, 18.0 Hz, 4-H_a), 3.93 (1H, dd, J = 12.8 Hz, 17.6 Hz, 4-H_b), 5.53 (1H, dd, J = 6.0 Hz, 12.0 Hz, 5-H), 6.71–7.43 (11H, m, 3′,4′,2″,3″,5″,6″, 2‴,3‴,4‴,5‴,6‴-H), 7.62 (1H, d, J = 4.8 Hz, 2'-H); ^{13}C NMR (100 MHz, DMSO-d_6) δ/ppm: 43.99 (-CH_2 of pyrazoline), 62.95 (-CH of pyrazoline), 113.42, 114.40, 116.17, 116.38, 119.28, 128.04, 128.09, 128.30, 128.34, 129.43, 129.48, 141.67 (-CH of aromatic region); 122.13, 132.45, 135.98, 144.26, 144.33 (-C of aromatic region); IR (KBr, 4000–400 cm^{-1}); 3078, υ (C–H)$_{ar\ stretching}$; 1589, υ (C=N); 1311, υ (C=C); 1149, υ (C–N); 1089, υ (C–Cl); 1003, 964, (*p*-substituted aromatic ring); 748, υ (C–H)$_{ar\ bending}$; 872, υ (C-S-C)$_{thiophene}$; Mass (*m/z*%): 338 (100) [M^+]; UV–vis: λ (nm) (ε, M^{-1} cm^{-1}): 269 (214800), 364 (262500).

5-(3-Chlorophenyl)-1-phenyl-3-(thiophen-2-yl)-4, 5-dihydro-1*H*-pyrazole (4f)

Prepared by above method using (E)-3-(3-chlorophenyl)-1-(thiophen-2-yl)prop-2-en-1-one (3f) (5 mmol, 1.24 g) and phenyl hydrazine (5 mmol, 0.49 mL). Yield: 83%; yellow crystalline solid. mp: 144–146 °C; mol. wt. 338.85 g mol^{-1}; anal. Calc. for: $C_{19}H_{15}ClN_2S$, calc. (found) (%): C, 67.35 (67.12); H, 4.46 (4.18); N, 8.27 (8.12); S, 9.46 (8.85); ^{1}H NMR (400 MHz, DMSO-d_6) δ/ppm: 3.17 (1H, dd, J = 5.6 Hz, 17.2 Hz, 4-H_a), 3.93 (1H, dd, J = 12.8 Hz, 18.4 Hz, 4-H_b), 5.53 (1H, dd, J = 6.4 Hz, 12.8 Hz, 5-H), 6.73–7.41 (11H, m, 3′,4′,2″,3″,4″,6″, 2‴,3‴,4‴,5‴,6‴-H), 7.62 (1H, d, J = 5.6 Hz, 2'-H); ^{13}C NMR (100 MHz, DMSO-d_6) δ/ppm: 44.00 (-CH_2 of pyrazoline), 63.03 (-CH of pyrazoline), 113.40, 116.31, 116.48, 119.37, 125.01, 126.26, 128.00, 128.11, 128.18, 128.31, 129.48, 131.52 (-CH of aromatic region); 133.98, 135.90, 136.98, 144.34, 144.36 (-C of aromatic region); IR (KBr, 4000–400 cm^{-1}); 3078, υ (C–H)$_{ar\ stretching}$; 1589, υ (C=N); 1311, υ (C=C); 1149, υ (C–N); 1089, υ (C–Cl); 941, (*m*-substituted aromatic ring); 748, υ (C–H)$_{ar\ bending}$; 872, υ (C-S-C)$_{thiophene}$; Mass (*m/z*%): 338 (100) [M^+]; UV–vis: λ (nm) (ε, M^{-1} cm^{-1}): 260 (67600), 374 (65800).

2.3.3 | General method of synthesis of complexes (5a-5f)

The square planar metal complexes (5a–5f) of type [Pd(4n)Cl_2] were synthesized by the reactions of Na_2PdCl_4 with the respective pyrazoline ligands (4a–4f) in a 1: 1 molar ratio in 1: 1 methanol chloroform system.

[Pd(4a)Cl_2] (5a)

A solution of ligand (4a) (0.191 g, 0.5 mmol), in chloroform, was added to methanolic solution of Na_2PdCl_4 (0.147 g, 0.5 mmol). The reaction mixture was refluxed for half an hour and then stirred 48 h at room temperature. Greenish brown product was obtained, which is filtered through whatman filter paper and washed with diethyl ether for several time then dried under reduced pressure. Proposed reaction is shown in Scheme 1. Yield: 69%; greenish brown solid. Mp: ≥ 300 °C; mol. Wt. 560.63 g mol^{-1}; anal. Calc. for: $C_{19}H_{15}BrCl_2N_2PdS$, calc. (found) (%): C, 40.71 (40.38); H, 2.70 (2.15); N, 5.00

(4.21); S, 5.72 (5.42); Pd, 18.98 (18.65); ^{1}H NMR (400 MHz, DMSO-d_6) δ/ppm: 3.12 (1H, dd, J = 7.2 Hz, 17.2 Hz, 4-H_a), 3.87 (1H, dd, J = 12.4 Hz, 16.8 Hz, 4-H_b), 5.25 (1H, dd, J = 7.2 Hz, 12.4 Hz, 5-H), 6.81–7.35 (11H, m, 3′,4′,2″,3″,5″,6″,2‴,3‴,4‴,5‴,6‴-H), 7.57 (1H, d, J = 4.8 Hz, 2'-H); ^{13}C NMR (100 MHz, DMSO-d_6) δ/ppm: 43.58 (-CH_2 of pyrazoline), 63.35 (-CH of pyrazoline), 113.18, 114.31, 116.58, 116.99, 119.29, 128.32, 128.38, 128.53, 128.58, 129.25, 129.36, 143.53 (-CH of aromatic region); 122.44, 132.48, 135.49, 144.15, 144.19 (-C of aromatic region); IR (KBr, 4000–400 cm^{-1}); 3070, υ (C–H)$_{ar\ stretching}$; 1612, υ (C=N); 1396, υ (C=C); 1172, υ (C–N); 1072, υ (C–Br); 1010, 980, (*p*-substituted aromatic ring); 779, υ (C–H)$_{ar\ bending}$; 902, υ (C-S-C)$_{thiophene}$; conductance: 09 Ω^{-1} cm^2 mol^{-1}; Mass (*m/z*): 560.6 [M^+]; UV–vis: λ (nm) (ε, M^{-1} cm^{-1}): 269 (91125), 390 (12563).

[Pd(4b)Cl_2] (5b)

It was synthesized using solution of ligand (4b) (0.191 g, 0.5 mmol). Yield: 61%; greenish brown solid. Mp: ≥ 300 °C; mol. Wt. 560.63 g mol^{-1}; anal. Calc. for: $C_{19}H_{15}BrCl_2N_2PdS$, calc. (found) (%): C, 40.71 (40.25); H, 2.70 (2.18); N, 5.00 (4.27); S, 5.72 (5.53); Pd, 18.98 (18.44); ^{1}H NMR (400 MHz, DMSO-d_6) δ/ppm: 3.17 (1H, dd, J = 6.8 Hz, 17.2 Hz, 4-H_a), 3.93 (1H, dd, J = 12.0 Hz, 17.6 Hz, 4-H_b), 5.52 (1H, dd, J = 6.0 Hz, 11.6 Hz, 5-H), 6.73–7.51 (11H, m, 3′,4′,2″,3″,4″,6″, 2‴,3‴,4‴,5‴,6‴-H), 7.72 (1H, d, J = 5.6 Hz,2'-H); ^{13}C NMR (100 MHz, DMSO-d_6) δ/ppm: 44.25 (-CH_2 of pyrazoline), 62.66 (-CH of pyrazoline), 113.49, 114.47, 119.35, 123.32, 128.14, 128.25, 128.32, 128.48, 129.43, 129.62, 130.95, 133.93 (-CH of aromatic region); 122.66, 125.47, 135.91, 144.47, 145.62 (-C of aromatic region); IR (KBr, 4000–400 cm^{-1}); 3070, υ (C–H)$_{ar\ stretching}$; 1558, υ (C=N); 1365, υ (C=C); 1172, υ (C–N); 1095, υ (C–Br); 910, (*m*-substituted aromatic ring); 779, υ (C–H)$_{ar\ bending}$; 840, υ (C-S-C)$_{thiophene}$; conductance: 10 Ω^{-1} cm^2 mol^{-1}; UV–vis: λ (nm) (ε, M^{-1} cm^{-1}): 264 (73563), 389 (16875).

[Pd(4c)Cl_2] (5c)

It was synthesized using solution of ligand (4c) (0.161 g, 0.5 mmol). Yield: 60%; greenish brown solid. Mp: ≥ 300 °C; mol. Wt. 499.72 g mol^{-1}; ^{1}H NMR (400 MHz, DMSO-d_6) δ/ppm: 3.13 (1H, dd, J = 6.0 Hz, 17.2 Hz, 4-H_a), 3.92 (1H, dd, J = 12.4 Hz, 17.6 Hz, 4-H_b), 5.52 (1H, dd, J = 6.0 Hz, 12.0 Hz, 5-H), 6.70–7.35 (11H, m, 3′,4′,2″,3″,4″,6″,2‴,3‴,4‴,5‴,6‴-H), 7.72 (1H, d, J = 4.8 Hz, 2'-H); ^{13}C NMR (100 MHz, DMSO-d_6) δ/ppm: 44.26 (-CH_2 of pyrazoline), 62.90 (-CH of pyrazoline), 113.58, 114.48, 116.23, 116.40, 119.32, 128.11, 128.34, 128.41, 128.50, 129.45, 129.60, 134.33 (-CH of aromatic region); 122.19, 138.94, 144.32, 144.47, 163.13 (-C of aromatic region); IR (KBr, 4000–400 cm^{-1}); 3070, υ (C–H)$_{ar\ stretching}$; 1605, υ (C=N); 1319, υ (C=C); 1157, υ (C–N); 1095, υ (C–Cl); 1003, 964, (*p*-substituted aromatic ring); 771, υ (C–H)$_{ar\ bending}$; 895, υ (C-S-C)$_{thiophene}$; conductance: 07 Ω^{-1} cm^2 mol^{-1}; UV–vis: λ (nm) (ε, M^{-1} cm^{-1}): 272 (71875), 394 (16563).

[Pd(4d)Cl_2] (5d)

It was synthesized using solution of ligand (4d) (0.161 g, 0.5 mmol). Yield: 71%; greenish brown solid. Mp: ≥ 300 °C; mol. Wt. 499.72 g mol^{-1}; ^{1}H NMR (400 MHz, DMSO-d_6) δ/ppm: 3.16 (1H, dd, J = 6.0 Hz, 17.2 Hz, 4-H_a), 3.94 (1H, dd, J = 12.0 Hz, 17.2 Hz, 4-H_b), 5.53 (1H, dd, J = 6.4 Hz, 12.0 Hz, 5-H), 6.72–7.43 (11H, m, 3′,4′,2″,3″,4″, 6″,2‴,3‴,4‴,5‴,6‴-H), 7.72 (1H, d, J = 5.2 Hz, 2'-H); ^{13}C NMR (100 MHz, DMSO-d_6) δ/ppm: 44.05 (-CH_2 of pyrazoline), 63.19 (-CH of pyrazoline), 113.39, 113.49, 114.76, 114.98, 119.35, 128.09, 128.15, 128.28, 128.43, 131.69, 131.79, 134.74 (-CH of aromatic region); 122.37, 135.91, 145.68, 145.77, 161.34 (-C of aromatic region); IR (KBr, 4000–400 cm^{-1}); 3070, υ (C–H)$_{ar\ stretching}$; 1566, υ (C=N); 1366, υ (C=C); 1157, υ (C–N); 1049, υ (C–Cl); 941, (*m*-substituted aromatic ring); 779, υ (C–H)$_{ar\ bending}$; 856, υ (C-S-C)$_{thiophene}$; conductance: 11 Ω^{-1} cm^2 mol^{-1}; UV–vis: λ (nm) (ε, M^{-1} cm^{-1}): 272 (78000), 378 (13365).

[Pd(4e)Cl_2] (5e)

It was synthesized using solution of ligand (4e) (0.169 g, 0.5 mmol). Yield: 65%; greenish brown solid. Mp: ≥ 300 °C; mol. Wt. 516.17 g mol^{-1}; anal. Calc. for: $C_{19}H_{15}Cl_3N_2PdS$, calc. (found) (%): C, 44.21 (43.92); H, 2.93 (2.41); N, 5.43 (5.02); S, 6.21 (5.95); Pd, 20.62 (20.14); ^{1}H NMR (400 MHz, DMSO-d_6) δ/ppm: 3.13 (1H, dd, J = 6.4 Hz, 18.0 Hz, 4-H_a), 3.93 (1H, dd, J = 12.8 Hz, 17.6 Hz, 4-H_b), 5.53 (1H, dd, J = 6.0 Hz, 12.0 Hz, 5-H), 6.71–7.43 (11H, m, 3′,4′,2″,3″,5″,6″,2‴,3‴,4‴,5‴,6‴-H), 7.69 (1H, d, J = 4.8 Hz, 2'-H); ^{13}C NMR (100 MHz, DMSO-d_6) δ/ppm: 43.94 (-CH_2 of pyrazoline), 62.65 (-CH of pyrazoline), 113.41, 114.45, 116.18, 116.34, 119.26, 128.05, 128.08, 128.33, 128.38, 129.47, 129.49, 144.14 (-CH of aromatic region); 122.15, 132.47, 135.90, 144.25, 144.36 (-C of aromatic region); IR (KBr, 4000–400 cm^{-1}); 3070, υ (C–H)$_{ar\ stretching}$; 1596, υ (C=N); 1365, υ (C=C); 1165, υ (C–N); 1095, υ (C–Cl); 1011, 972, (*p*-substituted aromatic ring); 741, υ (C–H)$_{ar\ bending}$; 933, υ (C-S-C)$_{thiophene}$; conductance: 07 Ω^{-1} cm^2 mol^{-1}; UV–vis: λ (nm) (ε, M^{-1} cm^{-1}): 271 (86938), 387 (12875).

[Pd(4f)Cl_2] (5f)

It was synthesized using solution of ligand (4f) (0.169 g, 0.5 mmol). Yield: 63%; greenish brown solid. Mp: ≥ 300 °C; mol. Wt. 516.17 g mol^{-1}; anal. Calc. for: $C_{19}H_{15}Cl_3N_2PdS$, calc. (found) (%): C, 44.21 (43.69); H, 2.93 (2.45); N, 5.43 (5.14); S, 6.21 (5.89); Pd, 20.62

(20.09); ^{1}H NMR (400 MHz, DMSO-d_6) δ/ppm: 3.17 (1H, dd, J = 5.6 Hz, 17.2 Hz, 4-H_a), 3.93 (1H, dd, J = 12.8 Hz, 17.6 Hz, 4-H_b), 5.53 (1H, dd, J = 6.4 Hz, 12.8 Hz, 5-H), 6.73–7.41 (11H, m, 3′,4′,2″,3″,4″,6″,2‴, 3‴,4‴,5‴,6‴-H), 7.72 (1H, d, J = 5.6 Hz, 2'-H); ^{13}C NMR (100 MHz, DMSO-d_6) δ/ppm: 44.10 (-CH_2 of pyrazoline), 63.43 (-CH of pyrazoline), 113.36, 116.28, 116.46, 119.52, 125.21, 126.35, 128.05, 128.12, 128.22, 128.30, 129.45, 135.38 (-CH of aromatic region); 131.62, 135.99, 136.53, 144.44, 144.48 (-C of aromatic region); IR (KBr, 4000–400 cm^{-1}); 3070, υ (C–H)$_{ar\ stretching}$; 1558, υ (C=N); 1373, υ (C=C); 1165, υ (C–N); 1095, υ (C–Cl); 887, (*m*-substituted aromatic ring); 732, υ (C–H)$_{ar\ bending}$; 925, υ (C-S-C)$_{thiophene}$; conductance: 09 Ω^{-1} cm^2 mol^{-1}; UV–vis: λ (nm) (ε, M^{-1} cm^{-1}): 271 (110100), 390 (7750).

2.4 | Biological application of synthesized compounds

2.4.1 | *In vitro* antibacterial activity

The *in vitro* antibacterial activity of free ligands and synthesized palladium (II) complexes was performed against two Gram positive(+ve): *Staphylococcus aureus*, *Bacillus subtilis* and three Gram negative(−ve): *Serratia marcescens, Escherichia coli, Pseudomonas aeruginosa* microorganisms. The experiment was performed according to literature procedure.[36,37]

2.4.2 | *In vitro* antimycobacterial activity

Determination of MIC of the test complexes against *M. tuberculosis* H_{37}Rv was performed by Lowenstein-Jensen agar (MIC) method.[38] The standard strain *M. tuberculosis* H_{37}Rv was tested with well-known drug rifampicin and isoniazide.[38,39]

2.4.3 | *In vitro* cytotoxicity using brine shrimp

In vitro cytotoxicity was performed according to our previously published literature.[40] Data were analyzed by simple logit method to determine the LC_{50} values, in which the log of concentration of samples were plotted against percentage of mortality of nauplii.

2.4.4 | *In vivo* cytotoxicity using *S. pombe*

The *in vivo* cytotoxicity was performed according to literature using *S. Pombe* cells.[41]

2.4.5 | Complex-DNA binding studies

Different techniques are used to find out complex-DNA interaction like spectroscopy, viscosity, circular dichroism, molecular modeling etc. Here, we have used absorption spectroscopy, viscosity and molecular modeling techniques for DNA binding studies.

Absorption titration technique

UV visible absorption titration is carried out using known concentration of Herring sperm DNA (HS DNA) in phosphate buffer and synthesized complexes (soluble in DMSO). HS DNA was dissolved in phosphate buffer and concentration of DNA is measured at 260 nm wavelength (ε = 12858 cm^{-1}). The experiment was carried out according to our previously published literature.[41]

Viscosity measurement

The hydrodynamic volume measurement study was carried out using an Ubbelohed viscometer kept under the thermostatic bath at constant temperature 27 ± 0.1 °C. The experiment was carried out according to literature.[42–44]

Ethidium bromide (EB) displacement method

Complexes exhibit no fluorescence at room temperature in solution or in the presence of HS DNA, and their binding to DNA could not be directly predicted through the emission spectra. Intense fluorescent light is emitted from EB in the presence of HS DNA due to the strong intercalation between adjacent DNA base pairs in the double helix; therefore, EB is considered to be a typical indicator of intercalation.[45] Hence, a competitive binding study of each complex with EB was done to understand whether the complex can displace EB from its HS DNA–EB complex and the mode of DNA interaction with the complexes. The HS DNA–EB complex was prepared by adding 33.3 μM EB and 10 μM HS DNA in buffer (phosphate buffer, pH 7.2). The possible intercalating effect of the complexes was studied by adding a certain amount of a solution of the complex step by step into a solution of the DNA–EB complex. The influence of the addition of each complex to the DNA–EB complex solution was obtained by recording the variation of fluorescence emission spectra with emission wavelength at 610 nm (excitation wavelength at 540 nm). The reaction time has been studied and the results showed that 4 min was enough for stabilization. So the change in fluorescence emission intensity was measured within 4 min after each addition. The values of the Stern–Volmer constant (K_{SV}, in M^{-1}) were calculated according to the linear Stern–Volmer equation (equation (2)) and the plots I_0/I vs. [Q].

$$I_0/I = K_{sv}\,[Q] + 1 \quad (2)$$

where I_0 is the emission intensity of EB-DNA in the absence of quencher (complex), I is the emission intensity of EB-DNA in the presence of quencher and [Q] is the quencher concentration.

To determine the strength of the interaction of complexes with DNA, the value of the binding constant (K_f) was calculated using the Scatchard equation (equation (3)):

$$\log \frac{(I0-I)}{I} = \log Kf + n\log[Q] \quad (3)$$

where I_0 and I are the fluorescence intensities of the EB-DNA in the absence and presence of different concentrations of complexes, respectively and n is the number of binding sites.

Molecular docking

To determine the theoretical binding energy of synthesized compounds to DNA, docking study was performed using HEX 6.0 software. The.pdb files of complex coordinates were obtained by converting their.mol file using CHIMERA 1.5.1 software. The structure of B-DNA (1 BNA: 5′-D(*CP*GP*CP*GP*AP*TP*TP*CP*GP*CP*G)-3′) obtained from the Protein Data Bank (http://www.rcsb.org/pdb). All solvents were removed before docking. Grid dimension 0.6 with FFT mode 3D and correlation type shape only were used. The other parameters kept at their default values.

Gel electrophoresis study

Gel electrophoresis have been performed to monitor cleavage of pUC19 DNA by synthesized complexes. The experiment was performed according to previously published literature procedure.[46]

3 | RESULTS AND DISCUSSION

3.1 | ^{1}H-NMR spectra, FT-IR, LC–MS spectra and EDX analysis

^{1}H-NMR of ligands (4a-4f) and complexes (5a-5f) are embedded in supplementary material 1a and 1b respectively. In ^{1}H-NMR spectra of ligands (4a-4f), three doublet of doublet between 3.00 to 5.50 δ ppm suggests the formation of 1,3,5-trisubstituted-4,5-dihydro-*1H*-pyrazole moiety. Peak around 7.60 ppm for ligands shifts to downfield in all complexes (5a-5f) indicates coordination of ligands to palladium (II). ^{13}C-NMR of ligands (4a-4f) and complexes (5a-5f) are embedded in supplementary material 2a and 2b respectively. In IR spectra of ligand 4a, bands observed at 1589, 1103 and 871 cm^{-1} are assigned to υ (C=N), υ (C–N) and υ (C-S-C), respectively. These bands are shifted to 1612, 1172 and 902 cm^{-1}, respectively in metal complex 5a. Similar trends is observed for IR spectra of all ligands (4a-4f) and metal complexes (5a-5f). The shift in above bands clearly indicates N and S atoms as the coordinating atoms. The IR spectral data are detailed in the experimental section.

Mass spectra of all ligands show corresponding molecular ion peak and data are embedded in the experimental section. Supplementary material 3 and 4 represents mass spectrum and probable fragments of complex 5a [Pd(4a)Cl_2]. Mass spectrum of complex 5a exhibits molecular ion peak [M^+] at 560.60 *m/z*, [M + 2] at 562.61 *m/z*, [M + 4] at 564.61 *m/z* and [M + 6] at 566.59, suggests the presence of two chlorine atoms and one bromine atom in the complex. The peak at 489.89 *m/z* is due to loss of two chlorine atoms from the complex 5a and peak at 383.25 *m/z* is due to the ligand attached with palladium (II). The peak at 306.18 m/z is due to the removal of phenyl ring from the fragmented ligand. The complexes have been characterized by EDX spectroscopy also, which is advantageous over C,H,N-elemental analysis, as we can determine the percentage of Cl, Br and metal ion along with C, H and N atoms. The EDX spectrum for complex 5a shows the existence of carbon, nitrogen, sulphur, chlorine, bromine and palladium elements (Figure 1) and confirmed the weight % of C, N, S, Cl, Br and Pd as 41.75, 5.47, 5.95, 12.89, 14.49 and 19.45%, as expected based on the calculated values of 40.71, 5.00, 5.72, 12.65, 14.25 and 18.98%, respectively.

3.2 | Thermogravimetric analysis

Thermogravimetric analysis is concerned with the change in weight of a material as its temperature changes. It indicates the temperature at which the material loses weight and weight loss indicates sample decomposition. The temperature, at which no weight loss occurs, reveals the stability of the material. TGA was carried out at a 10 °C per minute heating rate in the range of 20–800 °C under a nitrogen atmosphere. The characteristic thermogram of complex 5a shows two distinct mass losses

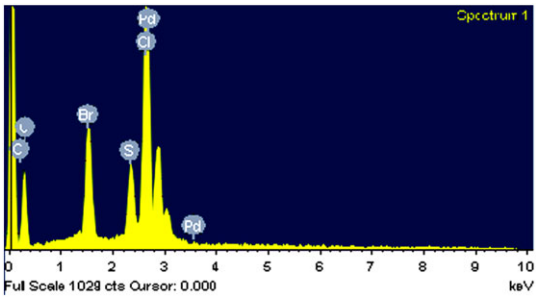

FIGURE 1 EDX spectrum of complex 5a

(supplementary material 5). The thermogram of complex 5a shows no weight loss up to ~200 °C, which infers the absence of lattice and coordinated water molecules. The mass loss (about 12%) during the first step between 200 and 350 °C corresponds to loss of two chlorine atoms from complex 5a. The second step (about 67%) corresponds to the decomposition of ligand and leaving behind the metal oxide as residue.[37]

3.3 | Magnetic moments, electronic spectra and conductance measurement

Magnetic moments measurement has been carried out at room temperature for all the Pd (II) complexes. Diamagnetic behaviour with zero B.M. μ_{eff} value of Pd (II) complexes suggests square planar geometry for all complexes. Electronic spectra of Pd (II) complexes have been recorded in DMSO. The absorption peaks are observed at around 300–390 nm and 200–280 nm, which can be assigned to d-d transition and metal to ligand charge-transfer transition (MLCT), respectively for square planar complexes.[47] To study the electrolytic nature of the palladium (II) complexes (5a-5f), their molar conductivities have been measured in DMSO. The molar conductance (Λ_M) values for the palladium (II) complexes are found in the range of 7–11 $cm^2\ \Omega^{-1}\ mol^{-1}$, indicating non electrolytic nature and absence of any counter ion outside the coordination sphere of the complexes. So, we conclude that all Pd (II) complexes are neutral in nature.

3.4 | Biological application of compounds

3.4.1 | *In vitro* antibacterial activity

The treatment of infectious diseases has been becoming an important and challenging problem because of emerging infectious diseases and emergence of inevitable antibiotic-resistant mutants among bacteria, which results in decreased efficacy and withdrawal of some antibiotic from widespread usage. Resistance to available antibiotics in pathogenic bacteria is currently a global challenge and hence, the substantial medical need for new classes of antimicrobial agents has been arising nowadays. The efficacy of the various organic therapeutic agents can often be enhanced upon coordination with a suitable metal ion. Hence, we have also evaluated the antibacterial activity of metal complexes against two Gram-negative bacterial strains: *E. coli* and *P. aeruginosa*; and against three Gram positive bacterial strains: *B. subtilis*, *S. aureus* and *S. marcescens* using the broth dilution method. *E. coli* cause gastrointestinal symptoms, ranging from mild to severe and bloody diarrhea, mostly without fever. *P. aeruginosa* can cause infection in lung, blood stream. Some *Bacillus* species can cause food poisoning. *S. marcescens* causes central nervous system diseases such as meningitis, urinary tract infection. Toxic shock syndrome (TSS) and staphylococcal scalded skin syndrome (SSSS) are associated with *S. aureus*.

The MIC (minimum inhibitory concentration) values are presented in supplementary material 6. The MIC values of all the ligands are in the range of 200 μM to 575 μM and complexes are in the range of 30 μM to 125 μM (Figure 2). The results reveal that most of the compounds exhibit significant antibacterial activity. Out of the twelve compounds, 5c, having electronegative F as a substituent atom at para position, displayed broad-spectrum antimicrobial activity against all tested bacterial strains with MIC values 30–75 μM. Moreover, compound 5a showed the most potent activity with MIC values of 35 μM for *B. subtilis* and 70 μM for *E. coli*. From the result, we can also conclude that chelation of heterocycle to metal also reinforce the antimicrobial activity of heterocyclic molecules.[48,49]

3.4.2 | *In vitro* antimycobacterial activity

The activity of the complexes against *M. tuberculosis* virulent strain $H_{37}Rv$ has been determined and results are presented in supplementary material 7. The fluorine substituted ligands containing complexes are more active against $H_{37}Rv$ strain than the other complexes. The highest MIC is found for the complexes 5c and 5d, having more electronegative F as a substituent atom. On the other hand, the least active complexes are the complex 5b (having bulkier and least electronegative Br as a substituent atom) and 5f, which exhibit MIC >250 μgmL^{-1}. But, all the compounds are less active than the standard drugs rifampicin and isonizaide.

3.4.3 | *In vitro* cytotoxicity using brine shrimp

Brine shrimp lethality bioassay is a useful tool to carry out *in vitro* cytotoxicity of compounds. The advantages

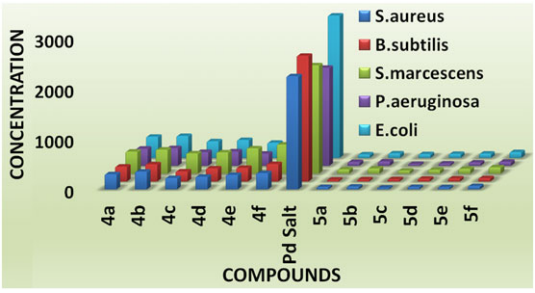

FIGURE 2 Minimal inhibitory concentration values of synthesized compounds

of this method include economical, less time consuming than other cytotoxicity test and more reliability. The assay has been carried out according to the protocol of Meyer *et al*.[50] A plot of log of sample concentration versus percentage of mortality has shown the linear relationship and the LC_{50} value of compounds have been calculated from the plot. The LC_{50} values of the compounds are in the range of 5.93 to 17.81 (supplementary material 7), which is comparable to cytotoxicity of reported Pd (II) complexes (LC_{50} = 6.83–15.93μgmL^{-1}).[51] The degree of mortality is directly proportional to the concentration of synthesized compounds. From the data recorded, complex 5c is the most potent amongst all the compounds. From Figure 3, it is concluded that the complexes are good cytotoxic agent than the ligands. The order of potency of compounds is 5c > 5d > 5e > 5f > 5a > 5b.

3.4.4 | *In vivo* cytotoxicity using *S. pombe*

Schizosaccharomyces pombe, the sixth model eukaryotic organism, has been used as an important organism in studying the cellular response to DNA damage and process of replication because many genes of this organism are homologous to human diseases genes.[52] Therefore, we have used this organism to carry out primary *in vivo* cytotoxicity test. The staining trypan blue dye could not penetrate through the live cell wall, but it could penetrate through the dead cell wall. Because of this, the dead *S. pombe* cells found to be blue in colour while live cells remain transparent under the microscope. Cellular level cytotoxicity of synthesized compounds on *S. pombe* cells has been carried out, in which trans platin and anticancer drug cisplatin have been used as the standard drugs. Result reflect that cytotoxicity is found proportional to the concentration of the compounds. The complexes show better cytotoxicity than reported pyrazoline based Ru (III) complexes.[53] Compounds 5c, 5d and 5e are found to have maximum cytotoxicity, while compounds 5a, 5b and 5f are found less cytotoxic (Figure 4). After 17 h of the treatment, many of the *S. pombe* cells died due to the toxic nature of the compounds (Figure 4). From experiment, it is observed that cytotoxicity of ligands are increased upon chelation with palladium (II).

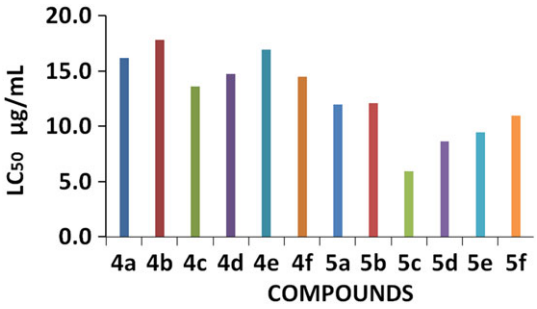

FIGURE 3 LC_{50} values in μgmL^{-1} of all compounds

3.4.5 | Complex-DNA binding

Absorption titration study

Among all the spectroscopic techniques, absorption titration study is very useful, prominent and reliable technique to study binding mode of small molecule to biopolymer like DNA. There are different kind of binding modes for interaction of small molecule with DNA. In this study, the binding mode of compounds to HS DNA has been determined. Absorption spectra are very sensitive to change in structure of compounds, and the structural change reflects in the absorption maxima. To determine the binding constant of synthesized compounds to HS DNA, we have monitoring the absorption maxima with gradual addition of DNA. For noncovalent interactioni.e., intercalation, hypochromism with or without red shift takes place.[54,55] While hyperchromism takes place in electrsostatic binding.[56] The observation of this study reflects the intercalative binding mode of compounds to HS DNA. The strong stacking interaction takes place between the DNA base pair and chromophoric group of the compound. The interaction slightly break the secondary structure of DNA, which causes the hypochromism.[57,58] Binding constant values for ligand-DNA interaction are in the range of 1.0×10^4 to 3.8×10^5 M^{-1}, while K_b values of complex-DNA interaction are in the range of 0.94×10^5 to 7.9×10^5 M^{-1}, which are comparable to antitumor drug cisplatin i.e. 5.51×10^4 M^{-1}, while higher than trans-platin i.e. 1.75×10^4 M^{-1} and lower than classical Intercalator EB

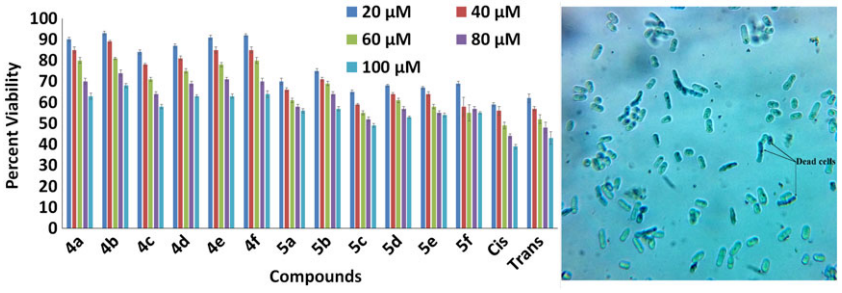

FIGURE 4 Cytotoxic effect of compounds on *S. Pombe* cells at five different concentration (Left) and *S. Pombe* cells after treatment with compound (Right)

i.e. 7×10^7 M^{-1}.[59,60] The binding strength of metal complexes with DNA are comparable to reported Pd complexes such as [Pd (H-Msal-mtsc) Cl (PPh_3)] (K_b = 1.44 x 10^5 M^{-1}), [Pd (H-Msal-metsc) Cl (PPh_3)] (K_b = 1.69 x 10^5 M^{-1})[61] and [(Pd (H-Msal-mtsc))$_2$(μ-ppm)] (K_b = 1.89 x 10^5 M^{-1});[62] while K_b values of complexes are higher than reported complexes such as [PdCl (dapdoH)] ($K_b = 4.6 \times 10^4$ M^{-1})[28] and [Pd (Msal-tsc)(PPh_3)] ($K_b = 5.0 \times 10^4$ M^{-1}).[61] The intrinsic binding constant K_b can be obtained from the ratio of slope to the intercept. (Figure 5).[63]

From the values of the binding constant (K_b), free energy (ΔG) of the compound–DNA complex has been calculated using equation (1):

$$\Delta G = -RT \ln K_b \quad (1)$$

Binding constants are the measure of the compound–DNA complex stability, while the free energy indicates the spontaneity or non-spontaneity of compound–DNA binding. The free energy value (ΔG = −26.00 to −33.66 kJmol^{-1}) of the Pd (II) complexes are negative. It indicates the spontaneity of compound–DNA interaction. Binding constant values and Gibb's free energy of complexes are higher than ligands. It indicates that upon complexation, binding ability of ligands enhances to a greater extent. Binding constants (K_b), free energy value (ΔG) and percentage hypochromism (%H = 1.07–20.10) of all compounds are shown in Table 1.

To calculate the interaction forces between the compound – HS DNA complex, the temperature dependant thermodynamic parametersi.e., change in enthalpy ($\Delta H°$), change in entropy ($\Delta S°$) and Gibb's free energy ($\Delta G°$) have been calculated using van't Hoff equation (equation (2)),[64] for complex 5b, which exhibit the highest binding constant.

$$\ln Kb = \frac{\Delta H^\circ}{RT} + \frac{\Delta S^\circ}{R} \quad (2)$$

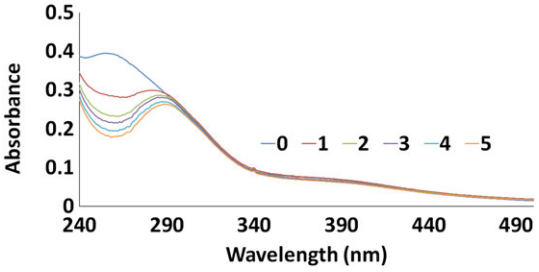

FIGURE 5 Absorption spectra upon addition of HS DNA to the solution of complex 5a after incubating for 10 minutes at room temperature in phosphate buffer (Na_2HPO_4/NaH_2PO_4, pH = 7.2). Inset: plot of [DNA]/ ($\varepsilon_a - \varepsilon_f$) vs. [DNA]

TABLE 1 Binding constant (K_b), percentage hypochromicity (%H), bathochromicity ($\Delta\lambda$), Gibb's free energy of all compounds

Compounds	K_b (M^{-1}) (× 10^5)	% H	$\Delta G°$(kJmol^{-1})
4a	0.10	11.67	−22.77
4b	0.10	7.71	−22.88
4c	0.14	1.07	−23.66
4d	0.20	9.77	−24.50
4e	0.72	5.77	−27.71
4f	0.36	8.31	−26.00
5a	1.32	11.78	−29.23
5b	7.49	22.84	−33.53
5c	1.58	9.73	−29.67
5d	1.53	8.82	−29.59
5e	0.94	17.76	−28.39
5f	2.45	15.40	−30.76

$$\Delta G^\circ = \Delta H^\circ - T\Delta S^\circ \quad (3)$$

where, K_b is the intrinsic binding constant measured at different absolute temperature (301.5, 303, 308, 313 K) and R is the gas constant in Jmol^{-1} K^{-1}. Enthalpy change and entropy change have been evaluated from the linear van't Hoff plot ($\ln K_b$ versus 1/T), where, slope gives $\Delta H°$ and intercept gives $\Delta S°$. The Gibb's free energy has been calculated from the equation (1), which is also verified by equation (3). All thermodynamic parameters for 5b-HS DNA complex are shown in Table 2, where negative values of $\Delta H°$ and $\Delta G°$ indicate that the interaction is thermodynamically favourable. The result shows that the binding may be driven by van der Waals forces and hydrogen binding, which is the main evidence for intercalative binding.[65]

Viscosity measurement

To support absorption titration, we have carried out relative viscosity measurement study. The viscosity of macromolecules are sensitive to their chain length and change in chain length. Intercalation and groove binding affect the length of DNA and hence the viscosity of DNA increases, while electrostatic binding does not affect the length of DNA and hence the viscosity of DNA remain constant.[66–68] Therefore, to clarify the mode of interaction of compounds to DNA, the change in relative viscosity of DNA with successive addition of has been measured. The relative viscosity of DNA has increased upon addition of free ligands as well as their respective complexes (Figure 6). Similar trend is observed for reported Pd complexes such as Pd (L)(PPh_3)], [Pd (L)($AsPh_3$)][69] and [PdCl (dapdoH)].[28] The insertion of

TABLE 2 Intrinsic binding constant (K_b), relative thermodynamic parameters of **5b** – HS DNA complex

T (K)	K_b ($\times 10^5$ M^{-1})	ΔG° (kJmol^{-1})	ΔH° (kJmol^{-1})	ΔS° (JK^{-1} mol^{-1})
301.5	7.49	−33.91	−47.98	−46.64
303	6.68	−33.79		
308	5.39	−33.79		
313	3.60	−33.29		

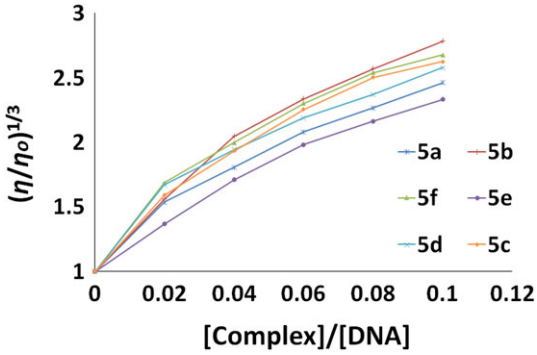

FIGURE 6 Effect on relative viscosity upon addition of complexes at 27 °C

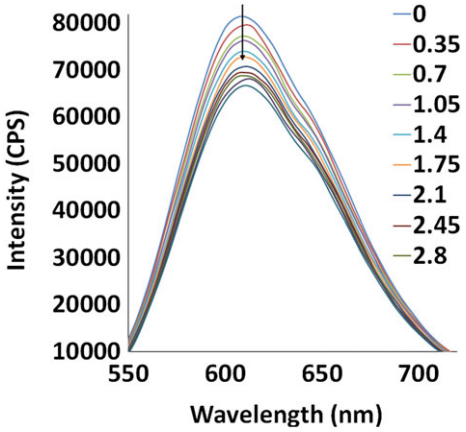

FIGURE 7 Emission spectra of EB-bound DNA solutions in the absence and presence of increasing concentrations of complex 5b (3.33–33.3 μM) in Tris–HCl. [EB] = 33.3 μM, [DNA] = 10.0 μM. The arrow shows the change in intensity upon increasing amounts of the complex

compound to the base pair of DNA results in lengthening of DNA chain due to the separation of base pair. This suggests intercalation mode of compounds to DNA binding.[70–73] Order of increase in viscosity for ligands is 4a < 4b < 4c < 4d < 4f < 4e and for complexes is 5e < 5a < 5d < 5c < 5f < 5b. This order is similar to the binding constant order of compounds.

Ethidium bromide (EB) displacement method

The successive addition of complexes 5a-5f to EB-DNA system at diverse "r" value [Complex]/ [DNA]) resulted in a remarkable decrease in fluorescence maxima of EB-DNA system (Figure 7). The displacement of EB by complexes, at 610 nm suggests the intercalative mode of complex to DNA binding. The extent of fluorescence intensity quenching is the measure of strength of binding between DNA and complexes.[74,75] In our study inner filter effect is corrected using Lakowics equation.[76] The observed fluorescence quenching data give a linear plot analogous to Stern-Volmer equation. The calculated quenching constant (K_{SV}) shows the ability of complexes to displace the EB.[77] The binding constant (K_f), quenching constants (K_{SV}), number of binding sites (n) are listed in Table 3. The K_f values calculated from Scatchard plots indicates that complex 5b exhibits the highest binding propensity and the order of binding strength of the complexes to HS-DNA is 5e < 5a < 5d < 5c < 5f < 5b, is same as observed in the UV titration study and viscosity measurement study. The K_f values of complexes are comparable to reported Pd complexes such as [Pd (DMEAIm^{iPr})Cl$_2$] (1.0 x 10^4 M^{-1}) and [Pd (DACH (Im^{iPr})$_2$)Cl$_2$] (2.0 x 10^4 M^{-1});[78] while K_f values are higher than reported Pd complexes such as [Pd (L)(PPh$_3$)] (3.92 x 10^3 M^{-1}) and [Pd (L)(AsPh$_3$)] (7.04 x 10^3 M^{-1}).[69] The values of "n" is observed around 1.0 indicates the 1: 1 molar ratio between the complexes and HS-DNA.

TABLE 3 Stern-Volmer quenching constant (K_{sv}), binding sites (n) and binding constant (K_f) from competitive

Complexes	K_{sv} (M^{-1})	Binding sites (n)	K_f (M^{-1})
5a	1.4×10^4	0.985	1.23×10^4
5b	7.0×10^3	1.255	1.22×10^5
5c	1.1×10^3	1.021	1.31×10^4
5d	6.4×10^3	1.052	1.24×10^4
5e	9.4×10^3	0.937	5.10×10^3
5f	9.0×10^3	1.144	4.18×10^4

Molecular docking

Molecular docking can provide some insight of the interactions of macromolecules with ligands and preferred

binding mode with the help of a variety of docking programs. To determine the relative binding energy of complex to DNA interaction, complexes have been docked to the B-DNA (PDB ID: 1BNA). In the docking method, out of 2000 docking solutions, only the lowest relative binding energy of docked structure has been obtained. From the ensuing docked structures it is clear that all compounds fit well into the rich G-C minor groove region of the targeted DNA, which is stabilized by van der Waals interaction and hydrophobic contacts. The representative docked structure is shown in Figure 8 and other docked structures are embedded in supplementary material 8. Relative binding energy of the docked structures of ligands are −251.16(4a); −255.92(4b); −257.95(4c); −261.89(4d); −269.11(4e) and − 267.73(4f) eV and of complexes are −252.61(5a); −260.86(5b); −254.38(5c); −253.61(5d); −251.60(5e) and − 258.24(5f) eV.

Gel electrophoresis

This experiment is carried out to measure the influence of complexes on the electrophoretic mobility and cleavage of the supercoiled form of pUC19 DNA in the absence of reducing agents.[79,80] The working principle of the gel electrophoresis is when circular plasmid DNA is subjected to electrophoresis, relatively fast migration will be observed for the intact supercoil form (Form I). If one strand of DNA is cleaved, the supercoiled form is relaxed to slower moving open circular or nicked form (Form II) and if both strands are cleaved linear form is generated which migrates in between the supercoiled (Form-I) and open circular form (Form-II).[81] Complexes have been found to promote the cleavage of pUC19 DNA from supercoiled Form I to the nicked Form II. As shown in Figure 9, the intensity of the circular supercoiled DNA (Form I) band is found to decrease, while that of the nicked (Form II) band apparently increase in lane 3 to 10. The gel electrophoretic separations shows the cleavage of pUC19 DNA induced by the complexes. The complexes 5c and 5e can induce the cleavage of the pUC19 DNA similar to cisplatin, and each lane has cleavage effect, comparing lanes 4–10 with lane 1, we can see the two complexes 5c and 5e have the highest cleavage percentage. Percentage cleavage of all compounds are embedded in supplementary material 9. Percentage comparison of DNA cleavage from SC form to OC form is shown in Figure 10.

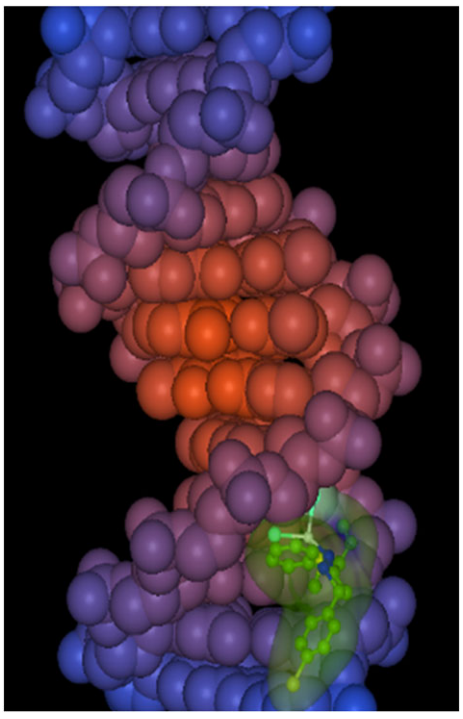

FIGURE 8 Molecular modeling of the complex 5a (ball and stick) with the DNA duplex (VDW spheres) of sequence (5′-D(*CP*GP*CP*GP*AP*AP*TP*TP*CP*GP*CP*G)-3′)

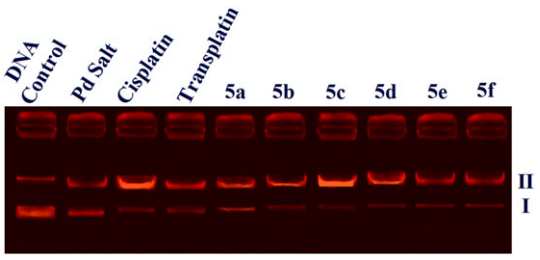

FIGURE 9 Photogenic view of cleavage of pUC19 DNA (300 μM) with a series of compounds using 1% agarose gel containing 0.5 μM EB, TE buffer (pH 8) at a final volume of 15 μL at 37 °C

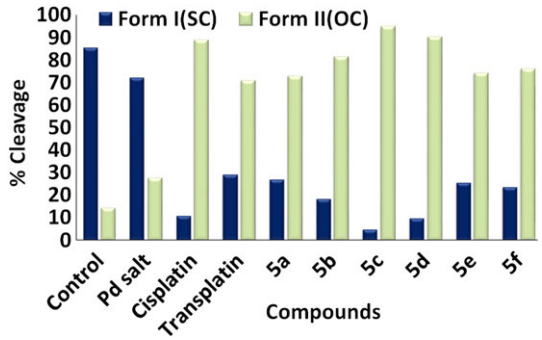

FIGURE 10 Percentage comparison of DNA cleavage from SC to OC form due to the influence of compounds

4 | CONCLUSION

Series of pyrazoline based palladium (II) complexes have been synthesized and characterized by various techniques. Chelating effect minimize high labiality and

hydrolysis rate of palladium complexes in the biological atmosphere and thus improve their biological activities. All compounds show noticeable antibacterial activity against five different microorganisms. Compounds with more electronegative fluorine substituted derivative give significant antimicrobial activity. Cytotoxicity studies using *brine shrimp* and *S. pombe* have been carried out and result suggest that fluorine substituted moiety is better cytotoxic agent than rest of five complexes. The results of absorption titration as well as viscosity measurement study suggest that all complexes bind to HS DNA via intercalative mode of binding. The binding constant of complexes are comparable to cisplatin and some reported complexes, while better than trans platin. The results of molecular docking and Gibb's free energy corroborated to both above studies. Also, all the thermodynamic parameters suggest the intercalative mode of complex to DNA binding. Fluorescence study provides additional evidence and suggest that metal complexes intercalate in between the stacks of DNA base pairs. Thus all the complexes bind to DNA via intercalative mode of binding and chelation helps to improve the binding strength of ligands to DNA. Complexes can efficiently cleave the plasmid DNA in absence of any external agents and this leads to the conclusion that hydrolytic cleavage mechanism involves in this study. Complexes 5c and 5d are compatible with cisplatin.

ACKNOWLEDGEMENTS

Authors are thankful to Head, Department of Chemistry, Sardar Patel University, India for making it convenient to work in laboratory, Dhanji P. Rajani, microcare laboratory, Surat for in vitro antimycobacterial activity and U. G.C., New Delhi for providing financial assistance of UGC BSR grant No. C/2013/BSR/Chemistry/59 and "BSR UGC One Time Grant", vide UGC letter No.F.19-119/2014 (BSR).

ORCID

Bhupesh S. Bhatt http://orcid.org/0000-0003-0693-3226
Mohan N. Patel http://orcid.org/0000-0001-9016-9245

REFERENCES

[1] F. Mancin, P. Scrimin, P. Tecilla, U. Tonellato, *Chem. Commun.* **2005**, 2540. https://doi.org/10.1039/B418164F

[2] J. V. Mehta, S. B. Gajera, D. D. Patel, M. N. Patel, *Appl. Organomet. Chem.* **2015**, *29*, 357.

[3] S. Satyanarayana, J. C. Dabrowiak, J. B. Chaires, *Biochemistry* **1992**, *31*, 9319.

[4] A. Sreedhara, J. A. Cowan, *JBIC J Biologic Inorganic Chem* **2001**, *6*, 337.

[5] L. H. Abdel-Rahman, R. M. El-Khatib, L. A. Nassr, A. M. Abu-Dief, M. Ismael, A. A. Seleem, *Spectrochim. Acta, Part A* **2014**, *117*, 366.

[6] A. M. Abu-Dief, L. A. Nassr, *J Iranian Chem Soc* **2015**, *12*, 943.

[7] L. H. Abdel-Rahman, A. M. Abu-Dief, R. M. El-Khatib, S. M. Abdel-Fatah, *Bioorg. Chem.* **2016**, *69*, 140.

[8] C. P. Raptopoulou, S. Paschalidou, A. A. Pantazaki, A. Terzis, S. P. Perlepes, T. Lialiaris, E. G. Bakalbassis, J. Mrozinski, D. A. Kyriakidis, *J. Inorg. Biochem.* **1998**, *71*, 15.

[9] R. Csonka, G. Speier, J. Kaizer, *RSC Adv.* **2015**, *5*, 18401.

[10] S. Dhar, M. Nethaji, A. R. Chakravarty, *Dalton Trans.* **2005**, 344.

[11] S. Dhar, D. Senapati, P. K. Das, P. Chattopadhyay, M. Nethaji, A. R. Chakravarty, *J. Am. Chem. Soc.* **2003**, *125*, 12118.

[12] G. Zhang, S. Shuang, C. Dong, D. Liu, M. M. F. Choi, *J. Photochem. Photobiol., B* **2004**, *74*, 127.

[13] C. J. Dhanaraj, J. Johnson, *Appl. Organomet. Chem.* **2016**, *30*, 860.

[14] A. Tanitame, Y. Oyamada, K. Ofuji, M. Fujimoto, K. Suzuki, T. Ueda, H. Terauchi, M. Kawasaki, K. Nagai, M. Wachi, J.-i. Yamagishi, *Bioorg. Med. Chem.* **2004**, *12*, 5515.

[15] A. A. Bekhit, H. M. A. Ashour, Y. S. Abdel Ghany, A. E.-D. A. Bekhit, A. Baraka, *Eur. J. Med. Chem.* **2008**, *43*, 456.

[16] Ş. Güniz Küçükgüzel, S. Rollas, H. Erdeniz, M. Kiraz, A. Cevdet Ekinci, A. Vidin, *Eur. J. Med. Chem.* **2000**, *35*, 761.

[17] D. Havrylyuk, B. Zimenkovsky, O. Vasylenko, L. Zaprutko, A. Gzella, R. Lesyk, *Eur. J. Med. Chem.* **2009**, *44*, 1396.

[18] N. R. Filipovic, S. Bjelogrlic, A. Marinkovic, T. Z. Verbic, I. N. Cvijetic, M. Sencanski, M. Rodic, M. Vujcic, D. Sladic, Z. Strikovic, T. R. Todorovic, C. D. Muller, *RSC Adv.* **2015**, *5*, 95191.

[19] B. Rosenberg, L. Van Camp, T. Krigas, *Nature* **1965**, *205*, 698.

[20] B. Rosenberg, L. Vancamp, J. E. Trosko, V. H. Mansour, *Nature* **1969**, *222*, 385.

[21] G. Chiara, M. Luigi, *Anti-Cancer Agents Med. Chem.* **2011**, *11*, 929.

[22] A. Bindoli, M. P. Rigobello, G. Scutari, C. Gabbiani, A. Casini, L. Messori, *Coord. Chem. Rev.* **2009**, *253*, 1692.

[23] C. Angela, M. Luigi, *Curr. Top. Med. Chem.* **2011**, *11*, 2647.

[24] H. Abd El-Halim, G. G. Mohamed, M. N. Anwar, *Appl. Organomet. Chem.* **2018**, 32.

[25] M. N. Alam, F. Huq, *Coord. Chem. Rev.* **2016**, *316*, 36.

[26] M. Fanelli, M. Formica, V. Fusi, L. Giorgi, M. Micheloni, P. Paoli, *Coord. Chem. Rev.* **2016**, *310*, 41.

[27] I. Eryazici, C. N. Moorefield, G. R. Newkome, *Chem. Rev.* **2008**, *108*, 1834.

[28] E. S. Koumousi, M. Zampakou, C. P. Raptopoulou, V. Psycharis, C. M. Beavers, S. J. Teat, G. Psomas, T. C. Stamatatos, *Inorg. Chem.* **2012**, *51*, 7699.

[29] G. Ayyannan, P. Veerasamy, M. Mohanraj, G. Raja, A. Manimaran, M. Velusamy, N. Bhuvanesh, R. Nandhakumar, C. Jayabalakrishnan, *Appl. Organomet. Chem.* **2017**, 31.

[30] K. Karami, S. Hashemi, J. Lipkowski, F. Mardani, A. A. Momtazi-borojeni, Z. M. Lighvan, *Appl. Organomet. Chem.* **2017**, 31.

[31] J. Schulz, A. K. Renfrew, I. Císařová, P. J. Dyson, P. Štěpnička, *Appl. Organomet. Chem.* **2010**, *24*, 392.

[32] W. Al Zoubi, A. A. S. Al-Hamdani, S. D. Ahmed, Y. G. Ko, *Appl. Organomet. Chem.* **2018**, 32.

[33] A. C. Ekennia, A. A. Osowole, D. C. Onwudiwe, I. Babahan, C. U. Ibeji, S. N. Okafor, O. T. Ujam, *Appl. Organomet. Chem.* **2018**, *32*, e4310.

[34] M. R. Mlahi, A. Negm, S. J. Azhari, M. M. Mostafa, *Appl. Organomet. Chem.* **2014**, *28*, 712.

[35] A. Rajini, A. K. Adepu, S. Chirra, N. Venkatathri, *RSC Adv.* **2015**, *5*, 66956.

[36] P. A. Vekariya, P. S. Karia, J. V. Vaghasiya, S. Soni, E. Suresh, M. N. Patel, *Polyhedron* **2016**, *110*, 73.

[37] L. H. Abdel-Rahman, N. M. Ismail, M. Ismael, A. M. Abu-Dief, E. A.-H. Ahmed, *J. Mol. Struct.* **2017**, *1134*, 851.

[38] A. Rattan, *Antimicrobials in laboratory medicine*, B. I. Churchill Livingstone Pvt. Ltd, New Delhi India. 1st edn., **2000**.

[39] D. Castagnolo, M. Radi, F. Dessì, F. Manetti, M. Saddi, R. Meleddu, A. D. Logu, M. Botta, *Bioorg. Med. Chem. Lett.* **2009**, *19*, 2203.

[40] M. N. Patel, C. R. Patel, H. N. Joshi, K. P. Thakor, *Spectrochim. Acta, Part A* **2014**, *127*, 261.

[41] J. V. Mehta, S. B. Gajera, M. N. Patel, *Med. Chem. Commun.* **2016**, *7*, 1367.

[42] M. N. Patel, B. S. Bhatt, P. A. Dosi, *Spectrochim. Acta, Part A* **2013**, *110*, 20.

[43] L. H. A. Rahman, A. M. Abu-Dief, N. A. Hashem, A. A. Seleem, *Int. J. Nano. Chem* **2015**, *1*, 79.

[44] L. H. Abdel-Rahman, A. M. Abu-Dief, E. F. Newair, S. K. Hamdan, *J. Photochem. Photobiol., B* **2016**, *160*, 18.

[45] B. C. Baguley, M. Le Bret, *Biochemistry* **1984**, *23*, 937.

[46] S. B. Gajera, J. V. Mehta, M. N. Patel, *RSC Adv.* **2015**, *5*, 21710.

[47] V. X. Jin, J. D. Ranford, *Inorg. Chim. Acta* **2000**, *304*, 38.

[48] B. Tweedy, *Phytopathology* **1964**, *55*, 910.

[49] M. N. Patel, S. H. Patel, M. R. Chhasatia, P. A. Parmar, *Bioorg. Med. Chem. Lett.* **2008**, *18*, 6494.

[50] B. N. Meyer, N. R. Ferrigni, J. E. Putnam, L. B. Jacobsen, D. E. Nichols, J. L. McLaughlin, *Planta Med.* **1982**, *45*, 31.

[51] M. N. Patel, A. P. Patidar, P. S. Karia, P. A. Vekariya, *Inorg. Chim. Acta* **2014**, *419*, 45.

[52] Wikipedia, *J.* **2016**.

[53] J. V. Mehta, S. B. Gajera, P. Thakor, V. R. Thakkar, M. N. Patel, *RSC Adv.* **2015**, *5*, 85350.

[54] Z.-C. Liu, B.-D. Wang, B. Li, Q. Wang, Z.-Y. Yang, T.-R. Li, Y. Li, *Eur. J. Med. Chem.* **2010**, *45*, 5353.

[55] M. N. Patel, B. S. Bhatt, P. A. Dosi, N. V. Amaravady, H. V. Movaliya, *Appl. Organomet. Chem.* **2012**, *26*, 217.

[56] L. Tjioe, A. Meininger, T. Joshi, L. Spiccia, B. Graham, *Inorg. Chem.* **2011**, *50*, 4327.

[57] M. N. Patel, D. S. Gandhi, P. A. Parmar, *Spectrochim. Acta, Part A* **2011**, *84*, 243.

[58] N. Chitrapriya, V. Mahalingam, M. Zeller, K. Natarajan, *Inorg. Chim. Acta* **2010**, *363*, 3685.

[59] C. N. N'Soukpoé-Kossi, C. Descôteaux, É. Asselin, H.-A. Tajmir-Riahi, G. Bérubé, *DNA Cell Biol.* **2007**, *27*, 101.

[60] M. J. Waring, *J. Mol. Biol.* **1965**, *13*, 269.

[61] P. Kalaivani, R. Prabhakaran, E. Ramachandran, F. Dallemer, G. Paramaguru, R. Renganathan, P. Poornima, V. V. Padma, K. Natarajan, *Dalton Trans.* **2012**, *41*, 2486.

[62] A. Shanmugapriya, G. Kalaiarasi, P. Kalaivani, F. Dallemer, R. Prabhakaran, *Inorg. Chim. Acta* **2016**, *449*, 107.

[63] A. Wolfe, G. H. Shimer, T. Meehan, *Biochemistry* **1987**, *26*, 6392.

[64] L. H. Abdel-Rahman, R. M. El-Khatib, L. A. Nassr, A. M. Abu-Dief, *J. Mol. Struct.* **2013**, *1040*, 9.

[65] Y. Zhang, G. Zhang, Y. Li, Y. Hu, *J. Agric. Food Chem.* **2013**, *61*, 2638.

[66] V. Rajendiran, M. Murali, E. Suresh, S. Sinha, K. Somasundaram, M. Palaniandavar, *Dalton Trans.* **2008**, 148. https://doi.org/10.1039/B710578A

[67] V. Rajendiran, M. Murali, E. Suresh, M. Palaniandavar, V. S. Periasamy, M. A. Akbarsha, *Dalton Trans.* **2008**, 2157. https://doi.org/10.1039/B715077F

[68] M. Inclán, M. T. Albelda, J. C. Frías, S. Blasco, B. Verdejo, C. Serena, C. Salat-Canela, M. L. Díaz, A. García-España, E. García-España, *J. Am. Chem. Soc.* **2012**, *134*, 9644.

[69] E. Ramachandran, P. Kalaivani, R. Prabhakaran, M. Zeller, J. H. Bartlett, P. O. Adero, T. R. Wagner, K. Natarajan, *Inorg. Chim. Acta* **2012**, *385*, 94.

[70] F. Dimiza, S. Fountoulaki, A. N. Papadopoulos, C. A. Kontogiorgis, V. Tangoulis, C. P. Raptopoulou, V. Psycharis, A. Terzis, D. P. Kessissoglou, G. Psomas, *Dalton Trans.* **2011**, *40*, 8555.

[71] C. Tan, J. Liu, H. Li, W. Zheng, S. Shi, L. Chen, L. Ji, *J. Inorg. Biochem.* **2008**, *102*, 347.

[72] L. H. Abdel-Rahman, A. M. Abu-Dief, R. M. El-Khatib, S. M. Abdel-Fatah, *J. Photochem. Photobiol., B* **2016**, *162*, 298.

[73] L. H. Abdel-Rahman, A. M. Abu-Dief, H. Moustafa, S. K. Hamdan, *Appl. Organomet. Chem.* **2017**, 31.

[74] A. Tarushi, K. Lafazanis, J. Kljun, I. Turel, A. A. Pantazaki, G. Psomas, D. P. Kessissoglou, *J. Inorg. Biochem.* **2013**, *121*, 53.

[75] G. Psomas, *J. Inorg. Biochem.* **2008**, *102*, 1798.

[76] J. R. Lakowicz, *Principles of Fluorescence Spectroscopy*, Springer US **2006**.

[77] G. H. Clever, Y. Söltl, H. Burks, W. Spahl, T. Carell, *Chem. – Eur. J.* **2006**, *12*, 8708.

[78] L. Massai, A. Pratesi, J. Bogojeski, M. Banchini, S. Pillozzi, L. Messori, Ž. D. Bugarčić, *J. Inorg. Biochem.* **2016**, *165*, 1.

[79] B. Macías, M. V. Villa, B. Gómez, J. Borrás, G. Alzuet, M. González-Álvarez, A. Castiñeiras, *J. Inorg. Biochem.* **2007**, *101*, 444.

[80] R. G. M. Moreno, M. V. Alipázaga, O. F. Gomes, E. Linares, M. H. G. Medeiros, N. Coichev, *J. Inorg. Biochem.* **2007**, *101*, 866.

[81] J. K. Barton, A. L. Raphael, *J. Am. Chem. Soc.* **1984**, *106*, 2466.

SUPPORTING INFORMATION

Additional supporting information may be found online in the Supporting Information section at the end of the article.

How to cite this article: Thakor KP, Lunagariya MV, Bhatt BS, Patel MN. Synthesis, characterization and biological applications of some substituted pyrazoline based palladium (II) compounds. *Appl Organometal Chem*. 2018;e4523. https://doi.org/10.1002/aoc.4523